Check for updates

Highly efficient and cheap treatment of dye by graphene-doped TiO_2 microspheres

Honglian Liang, Shujun Wang, Yanhong Lu, Ping Ren, Guihua Li, Fenghao Yang and Yu Chen

ABSTRACT

Highly efficient dye wastewater treatment by photocatalytic catalysis commonly requires expensive catalysts, long degradation time and a complicated procedure. Here, we for the first time prepared cheap graphene-doped titanium dioxide microspheres with a simple procedure to degrade dye with high efficiency. When the catalyst concentration was 0.2 $g{\cdot}L^{-1}$, the photocatalysis degradation extent of methylene blue solution, methylene green solution and 1,9-dimethyl methylene blue solution reached 96.4, 85.9 and 98.7%, respectively. The results showed that the degradation reactions accorded with the Langmuir–Hinshelwood model, and the photocatalytic reactions belonged to a first-order reaction in the primary stage. Furthermore, different photocatalytic degradation mechanisms were proposed, which have not been found in other literature. This work opened a new route for simple preparation of cheap microspheres in photocatalytic dye wastewater treatment with high efficiency.

Key words | composite microspheres, dye wastewater, graphene, titanium dioxide, treatment

Honglian Liang (corresponding author)
Shujun Wang
Yanhong Lu
Ping Ren
Guihua Li
Fenghao Yang
Yu Chen
Department of Chemistry and Material Science,
Langfang Normal University,
Langfang 065000, Hebei,
China
E-mail: *lianghonglian@lfnu.edu.cn*

HIGHLIGHTS

- Graphene-doped TiO_2 microspheres were prepared for the first time.
- Degradation of three dye solutions was cheap and efficient, with the composites showing recyclability for their reuse.
- Different photocatalytic degradation mechanisms for the three solutions were proposed.

GRAPHICAL ABSTRACT

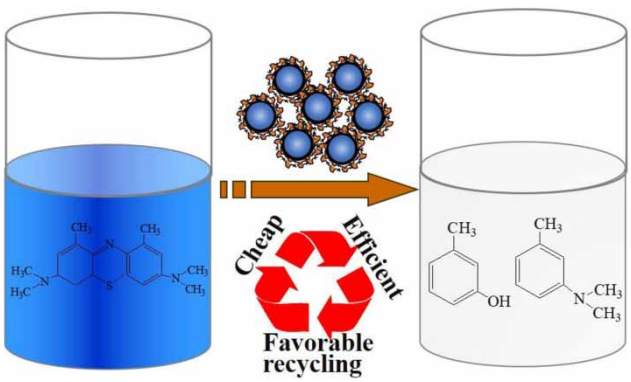

doi: 10.2166/wst.2020.545

Downloaded from http://iwaponline.com/wst/article-pdf/83/1/223/834977/wst083010223.pdf
by guest

INTRODUCTION

With the rapid development of industry, the problem of water pollution is severe, and efficient treatment of dye wastewater has become one of the problems to be solved urgently. In recent years, micro-nano microspheres have been widely used in the fields of photocatalytic degradation due to their unique photoelectric properties, controllable size and biocompatibility (Wang *et al.* 2013; Baschir *et al.* 2019; Xiao *et al.* 2019). The template method is the most extensive and effective method for the preparation of micro-nano microspheres. Its advantage lies in that it can design templates according to the size, morphology and properties of the prepared materials, and the template can be designed by tuning the spatial limitation and regulation effect (Zhi *et al.* 2005; Wei *et al.* 2009; Acharya *et al.* 2010). Among all kinds of templates, a silicon dioxide (SiO_2) template was widely used in the preparation and performance research of microsphere materials because of low cost, good dispersibility, high stability and easy functionalization (Pal *et al.* 2014a, 2014b; Elma *et al.* 2015; Nador *et al.* 2017; Ette *et al.* 2018).

Nano titanium dioxide (TiO_2) has become one of the research hotspots of environmental protection and pollution abatement due to its advantages of non-toxicity, good stability, and high photocatalytic efficiency (Zhang *et al.* 2015; Shakeel *et al.* 2016; Bai *et al.* 2020). However, the disadvantages of TiO_2 (such as slow transfer rate between photoelectron and hole, high recombination rate and low light utilization rate) limit the application and development in photocatalytic fields. It has been discovered that doping and modification could effectively inhibit the agglomeration and improve the photocatalytic activity of nano TiO_2 (Zhang & Zhang 2009; Nguyen *et al.* 2011; Juma *et al.* 2016). Nano TiO_2 powder is easy to be suspended and agglomerated, and difficult to be recovered and utilized. Compared with nano TiO_2, micro-nano TiO_2 microsphere material has good rheological property, favorable cycle performance and strong adsorption ability that can remove the pollutants from the wastewater. Therefore, micro-nano TiO_2 microsphere material shows greater advantages in the field of photocatalysis (Liu *et al.* 2010, 2020; Tang *et al.* 2013; Kim *et al.* 2017).

We prepared the graphene-doped TiO_2 microspheres and used them to degrade methylene blue solution, methylene green solution and 1,9-dimethyl methylene blue solution with high photocatalysis degradation rates for the first time. Furthermore, the products of photocatalytic degradation of the three dye solutions were analyzed, and the possible photocatalytic degradation mechanisms were proposed. The degradation mechanisms of the three solutions were never found in other literature, to the best of our knowledge. The prepared microsphere material showed bright application prospect and research value in dye wastewater treatment, functional materials and many other fields.

MATERIAL AND METHODS

Materials

Graphene (>99%) was purchased from Stremchemical Inc. USA, and aminopropyl triethoxysilane (KH550, >98%) was purchased from Shanghai Tixi Aihuacheng Industry Co. Ltd. SiO_2 template microspheres were made in the laboratory. Butyl titanate, methylene blue, methylene green, and anhydrous ethanol (AR) were purchased from Tianjin Damao Chemical Reagent Factory. 1,9-dimethyl methylene blue (GR) was purchased from Beijing Huamaike Biotechnology Co. Ltd.

Synthesis of graphene-doped TiO_2 microspheres

At room temperature of 25 °C, 0.2 g SiO_2 template microspheres and 0.1 g KH550 were dispersed in 25 mL anhydrous ethanol and stirred magnetically for 30 min to form mixed suspension A. Then, the mixture suspension B composed of 1 mL butyl titanate and 5 mL anhydrous ethanol was added to the mixture suspension A with a rate of 2–3 seconds/drop. Then, the mixed suspension was refluxed at 80 °C for 100 min. The prepared products were washed with water and anhydrous ethanol, dried at 50 °C, and calcined at different temperatures for 2 h. Lastly, the products were placed in 20 mL 0.3 mol·L^{-1} NaOH solution and refluxed at 85 °C for 1.5 h to obtain TiO_2 microspheres. In the same way, a certain amount of graphene was added into solution A to prepare graphene-doped TiO_2 microspheres with different graphene doping ratios.

Characterization

The surface morphology and microstructure of the graphene-doped TiO_2 microspheres were characterized by scanning electron microscopy (SEM, Quanta FEG 250,

Downloaded from http://iwaponline.com/wst/article-pdf/83/1/223/834977/wst083010223.pdf
by guest

USA) and transmission electron microscopy (TEM) with a Japan JEM-2100F transmission electron microscope. The crystal structure of graphene-doped TiO_2 microspheres was characterized by X-ray diffraction (XRD) using a D8 Advance (Bruker-AXS) X-ray diffractometer with Cu Ka radiation ($\lambda = 0.1546$ nm). The UV-visible diffuse reflectance spectra (UV-Vis DRS) of graphene-doped TiO_2 microspheres were recorded by a spectrophotometer (UV-2550, Shimazu, Japan). The surface elements and ionic valence states of the graphene-doped microspheres were analyzed by a Japan Kratos Axis Supra X-ray photoelectron spectrometer (XPS). The optical power density of a xenon lamp was measured by an optical power meter (CEL-NP2000, China). The degradation products of the three dyes were analyzed by two-dimensional liquid chromatography–ion trap mass spectrometry (LC-MS, Agilent 1100, USA). A CAPCELL PAK C18 column was used to isolate and the column temperature was 35 °C. The mobile phase was ammonium acetate (0.1% formic acid), acetonitrile and methanol (2 mmol·L^{-1}) with the flow rate of 350 L·min^{-1}. The injection quantity was 10 L. The absorbances of the three dyes were analyzed using a visible spectrophotometer (722, Shanghai Optical Instrument Factory).

Photocatalytic activity test

Fifteen milligrams of graphene-doped TiO_2 microspheres was added to 100 mL methylene blue solution, methylene green solution and 1,9-dimethyl methylene blue with the concentration of 10, 12, 15 and 20 mg·L^{-1}. The samples were magnetically stirred for 2 h in dark condition to achieve adsorption–desorption equilibrium. Then, the photocatalytic degradation experiments were conducted under a xenon lamp, and the xenon lamp was placed 15 cm away from the surface of the solutions. The optical power density of the xenon lamp was 752 MW·cm^{-2}. At given time intervals, 3 mL aliquots were sampled and centrifuged to remove photocatalyst powders. The filtrates were analyzed using a visible spectrophotometer, and the absorbances were recorded at the maximum absorption wavelength of 664, 589 and 647 nm, respectively. The degradation efficiencies were calculated as Equation (1).

$$\text{Degradation rate } (\%) = \frac{A_0 - A}{A_0} \times 100 \quad (1)$$

A_0 and A represent initial absorbance and absorbance after degradation, respectively.

RESULTS AND DISCUSSION

Characterization results

Figure 1(a) and 1(b) show SEM and TEM images of graphene-doped TiO_2 microspheres, respectively. From the SEM images, we found that the prepared microspheres had a regular spherical morphology with a diameter around 1 micron and a relatively uniform particle size distribution, but no agglomeration. According to the results of TEM, the tulle-like graphene with three-dimensional network on the surface of microspheres can be found. We speculate that graphene hindered the agglomeration of graphene-doped TiO_2 microspheres, facilitated the adsorption and rapid decomposition of pollutants, and provided a transport channel for the rapid separation of photogenerated electron-hole pairs in the photocatalytic degradation process.

The prepared graphene-doped TiO_2 microspheres (1.5% graphene, calcined at 500 °C) were characterized by XRD. As shown in Figure 1(c), typical diffraction peaks are located at $2\theta = 25.8$, 37.8, 49.9, 55.7 and 64.5°, corresponding to the crystal planes (101), (004), (200), (211) and (204) of anatase TiO_2. However, no characteristic diffraction peak of graphene was found because the content of graphene in the composite microspheres was low, or the diffraction peak of graphene around 26.0° was covered by the diffraction peak of TiO_2. The doping of graphene was later verified using XPS analyses (Figure 2).

Figure 1(d) shows the UV-Vis DRS of TiO_2 P25 and graphene-doped TiO_2 microspheres. From the Figure 1(d), we found that the graphene-doped TiO_2 microsphere had a red shift and the absorption of visible light in the visible light band of 400–600 nm compared with P25 TiO_2. The absorption sideband was estimated to be about 440 nm by tangent epitaxial method. The band gap energy (Eg) of the microsphere can be calculated using the formula $Eg = 1{,}240/\lambda$. The band gap energy of TiO_2 in the microspheres is 2.8 eV, which is 0.3 eV lower than P25 TiO_2. Graphene had high conductivity and the resonance effect of sp2 hybrid carbon was enhanced under visible light excitation. At the same time, graphene could promote the effective separation of cavity-electron pairs of TiO_2 as the capture center

Downloaded from http://iwaponline.com/wst/article-pdf/83/1/223/834977/wst083010223.pdf
by guest

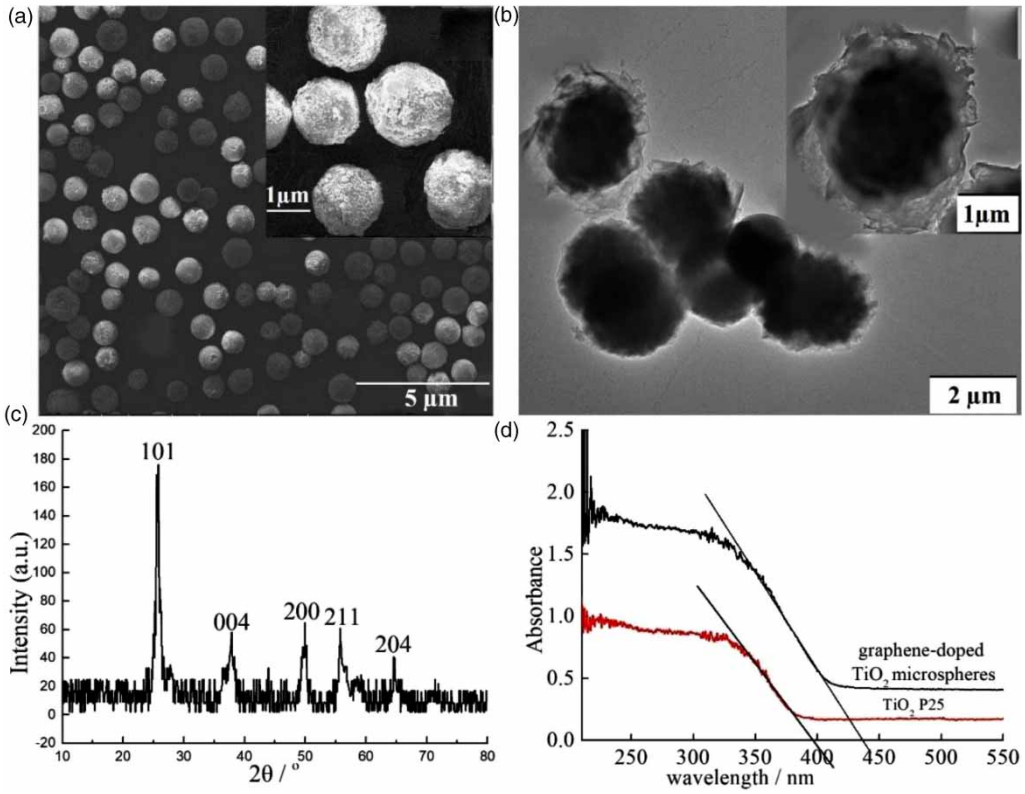

Figure 1 | Characterization results of the graphene-doped TiO_2 microspheres: (a) SEM, (b) TEM, (c) XRD, (d) UV-Vis DRS.

of electrons in the photocatalytic reaction process (Yu *et al.* 2016; Kim *et al.* 2019; Pant *et al.* 2020).

Figure 2 shows the XPS spectra of graphene-doped TiO_2 microspheres. As shown in Figure 2(a), the graphene-doped TiO_2 microspheres were mainly composed of Ti, O and C. The binding energies of Ti 2p3/2 and Ti 2p1/2 of the graphene-doped TiO_2 microspheres were 458.7 and 464.4 eV in Figure 2(b), indicating that Ti element existed in the form of Ti^{4+}. In Figure 2(c), the binding energies of the graphene-doped TiO_2 microspheres in the C1s orbit were derived from C=C and C-C, C-OH, C=O, O=C-OH and other functional groups in graphene. In Figure 2(d), the diffraction peaks of the O1s orbit were C-O bond and Ti-O bond (Nappini *et al.* 2017; Shinde *et al.* 2018; Bagus *et al.* 2019).

Determination of photocatalytic performance

The influences of doping ratio, calcination temperature, material usage and time on the degradation rate were explored in the photocatalytic degradation experiments. From Figure 3(a)–3(c), we found that the graphene-doped TiO_2 microspheres (1.5% graphene, calcined at 500 °C) had a very high photocatalytic activity for the three solutions with the concentration 10 mg·L^{-1}, and the photocatalysis degradation extent reached 96.4, 85.9 and 98.7%, respectively. More importantly, the time taken by the graphene-doped TiO_2 microspheres to reach the degradation equilibrium for the three dyes varied greatly. Figure 3(d)–3(f) show that the degradation rate of methylene blue and 1,9-dimethyl methylene blue basically reached the maximum at 120 and 60 min, respectively. But the degradation rate of methylene green reached the maximum at 8 min. We speculated that a possible cause is the degradation product was adsorbed on the surface of the microspheres, blocking the pore channel and making the catalyst inactivated. Li and colleagues synthesized polypyrrole-modified granular activated carbon composites (PPy/granular activated carbon) and used them to adsorb methyl tert-butyl (MTB). The adsorption of PPy/GAC for MTB was very rapid, and adsorption equilibrium was reached in about 10 minutes. They speculated the possible reason was that the MTB after being adsorbed blocked the pores of the composites (Li *et al.* 2017). He and colleagues prepared Zn-Co/AC catalysts and applied them in an acetylene acetoxylation reaction. The Zn-Co/AC with different Co addition ratio exhibited relatively high catalytic activity, and the CH_3COOH conversion stopped after 3 h (He *et al.* 2018). It is also consistent with the conclusion from the degradation results as a function of the time in

Downloaded from http://iwaponline.com/wst/article-pdf/83/1/223/834977/wst083010223.pdf
by guest

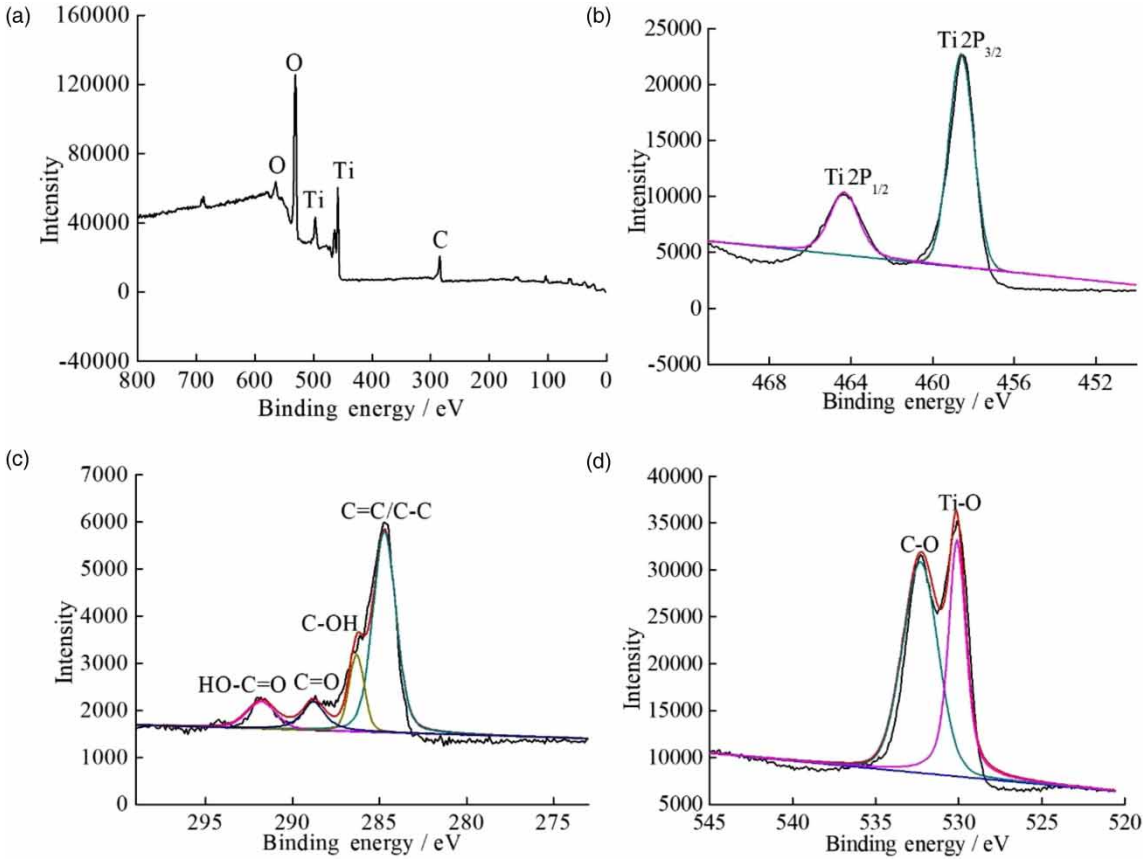

Figure 2 | XPS spectra of graphene-doped TiO_2 microspheres.

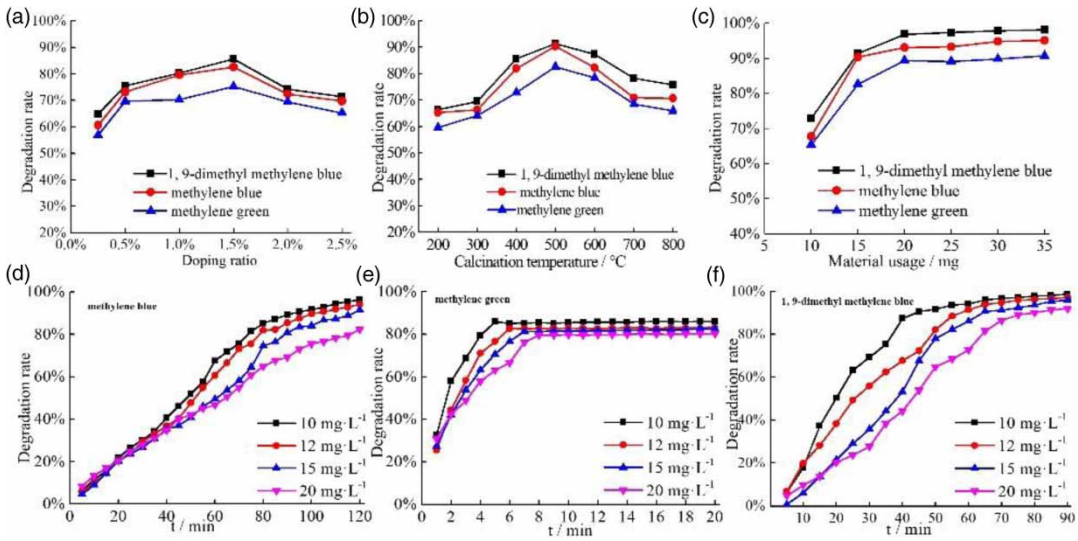

Figure 3 | The influence of various factors on the degradation rate: (a) doping ratio, (b) calcination temperature, (c) material usage, (d)–(f) time.

our work. Therefore, we speculated that the degradation products blocked the pore channel of the microspheres and inactivated the catalyst, and the degradation of methylene green stopped at 86% after 10 min. As a matter of fact, the data of Figure 3 can be easily explained by the fact that the presence of the nitro group renders the molecule skeleton

Downloaded from http://iwaponline.com/wst/article-pdf/83/1/223/834977/wst083010223.pdf
by guest

more sensitive than the NO_2-free molecules. Therefore, it was speculated that the degradation process of methylene green was different from the other two dyes due to the influence of the nitro functional group.

Photocatalytic kinetics

Currently, the photocatalytic reaction model used for photocatalytic reaction kinetics is the Langmuir–Hinshelwood model (Equation (2)) (Michael *et al.* 2013; Pham *et al.* 2014; Anas *et al.* 2015).

$$r = -\frac{dc}{dt} = \frac{k_r K_a c}{1 + K_a c_0} = Kc \quad (2)$$

r: rate of photocatalytic reaction
c: concentration of organic matter
c_0: initial concentration of organic matter
k_r: reaction rate constant
K_a: equilibrium adsorption constant
K: apparent rate constant.

The obtained data of graphene-doped TiO_2 microspheres (1.5% graphene, calcined at 500 °C) to degrade the three solutions with concentrations of 10, 12, 15 and 20 mg·L^{-1} were fitted linearly. Figure 4 shows that at the initial stages of the photocatalytic reactions (methylene blue and 1,9-dimethyl methylene blue within 30 min, methylene green within7 min), the linear relationships of the obtained lines were good, and R^2 values were above 0.99 (Table 1). According to the data in Table 1, we could make the following conclusions. (1) The photocatalytic degradation extent constant (K) of the three dyes by graphene-doped TiO_2 microspheres decreased with the increase of the dye concentration, which was consistent with literature reports (Michael *et al.* 2013; Pham *et al.* 2014; Anas *et al.* 2015). (2) In the primary reaction stage, the order was $K_{\text{methylene green}} > K_{\text{1,9-dimethyl blue}} > K_{\text{methylene blue}}$, indicating that the degradation extent of methylene green was higher than the other two dyes. However, since the degradation rate of methylene green almost did not change after 10 minutes, the final degradation extent of methylene green was the lowest among the three dyes. (3) The sequence of photochemical reaction extent for the three dyes was $r_{\text{methylene green}} > r_{\text{1,9-dimethyl blue}} > r_{\text{methylene blue}}$, and the photochemical reaction extents were much higher than those reported in the literature (Pare *et al.* 2016; Cabir *et al.* 2017; Yang *et al.* 2018).

Contrast experiment and photocatalytic stability

Comparison experiments

The photocatalytic properties of TiO_2 P25, TiO_2 microspheres and graphene-doped TiO_2 microspheres were compared in the comparision experiments. The experimental results in Table 2 showed that (1) the degradation extent sequence of different catalysts was graphene-doped TiO_2 microsphere > TiO_2 microsphere > P25; compared with TiO_2 P25, the degradation extent of graphene-doped TiO_2 microspheres for the three solutions increased more than 30% on average; (2) the degradation extent sequence for the three dyes was 1,9-dimethyl methylene blue (120 min) > methylene blue (10 min) > methylene green (60 min).

Photocatalytic stability

To evaluate the photocatalytic stability of the graphene-doped TiO_2 microspheres, the same photocatalytic experiments were repeated for eight times. Specifically, the samples were filtered using a filter membrane, and

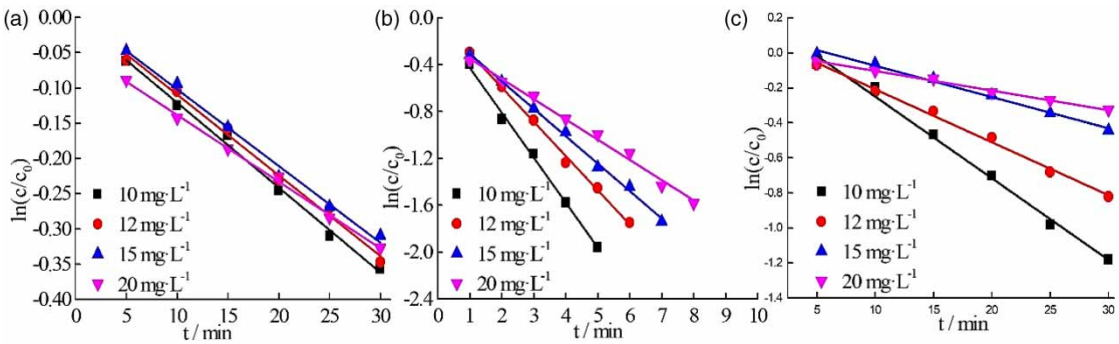

Figure 4 | The fitted curves of first-order reaction: (a) methylene blue, (b) methylene green, (c) 1,9-dimethyl methylene blue.

Downloaded from http://iwaponline.com/wst/article-pdf/83/1/223/834977/wst083010223.pdf
by guest

Table 1 | The kinetic fitting data of first-order reaction of catalyst with different concentration

Dye	Concen./mg·L^{-1}	Kinetic equation	K/min^{-1}	R^2	r/mol·g^{-1}·h^{-1}
Methylene blue	10	$y = -0.01205 \times 0.0003146$	0.01205	0.9937	75.3
	12	$y = -0.01145x + 0.00514$	0.01145	0.9908	88.2
	15	$y = -0.01089x + 0.00704$	0.01089	0.9903	107.2
	20	$y = -0.00946x - 0.04365$	0.00946	0.9974	150.6
Methylene green	10	$y = -0.3839x - 0.04$	0.3839	0.9954	591.8
	12	$y = -0.2924x - 0.00797$	0.2924	0.9965	688.8
	15	$y = -0.2343x - 0.07171$	0.2343	0.9965	846.7
	20	$y = -0.17284x - 0.17408$	0.17284	0.9905	1103.1
1,9-dimethyl methylene blue	10	$y = -0.04663x + 0.21726$	0.04663	0.9912	113.3
	12	$y = -0.0302x + 0.09467$	0.03022	0.9931	131.9
	15	$y = -0.01787x + 0.010567$	0.01787	0.9901	155.3
	20	$y = -0.0112x + 0.00948$	0.0112	0.9936	174.8

Table 2 | Photocatalytic performance comparison of different catalysts

Catalyst	Methylene blue	Methylene green	1,9-dimethyl methylene blue
P25	70.2%	62.1%	75.4%
TiO_2 microsphere	76.3%	65.2%	85.3%
Graphene-doped TiO_2 microsphere	96.4%	85.9%	98.7%

graphene-doped TiO_2 microspheres were washed by distilled water and dried after the photocatalytic experiment. The recovery and leakage of the microspheres were 96 and 4%. Figure 5 shows the results of the recycling experiments. As observed from Figure 5, the degradation extent of methylene green solution was reduced by just 2% after eight repetitive cycles of photodegradation experiments. Meanwhile, the degradation extent of methylene blue and 1,9-dimethyl methylene blue solution still remained more than 90%, indicating that the graphene-doped TiO_2 microspheres were relatively stable during the photocatalytic reaction. In addition, the graphene-doped TiO_2 composites were micron-sized and precipitated quickly, so they could be separated and recycled easily from the working solution. This result demonstrated that the had excellent chemical stability and could serve as recyclable photocatalytic material for many practical applications.

Degradation products and mechanism speculation

The degradation products of the three dyes with the concentration of 10 mg·L^{-1} under optimal conditions (1.5% graphene, calcined at 500 °C) were analyzed by LC-MS, and the results are shown in Figure 6. According to the LC-MS data in Figure 6, the photocatalytic degradation processes of three dye molecules were proposed (Figure 7). As can be seen from Figure 6(a), in addition to the peak of residual methylene blue ($m/z = 284.2$), there were many other small molecule peaks of methylene blue degradation: 2-amino-benzene sulfonic acid ($m/z = 173.3$), benzene sulfonic acid ($m/z = 158.8$) and phenol ($m/z = 94$). The photocatalytic degradation process of 1,9-dimethyl methylene blue (Figure 7(b)) was similar to that of methylene

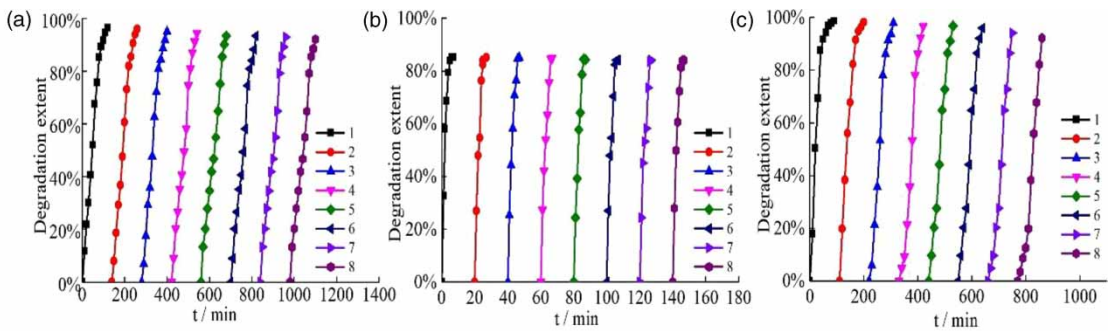

Figure 5 | The recycling experiments for three solutions: (a) methylene blue, (b) methylene green, (c) 1,9-dimethyl methylene blue.

Downloaded from http://iwaponline.com/wst/article-pdf/83/1/223/834977/wst083010223.pdf
by guest

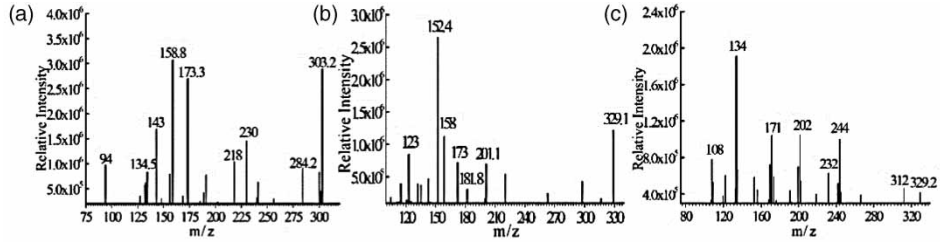

Figure 6 | LC-MS spectra of degradation products for three dye molecules: (a) methylene blue, (b) methylene green, (c) 1,9-dimethyl methylene blue.

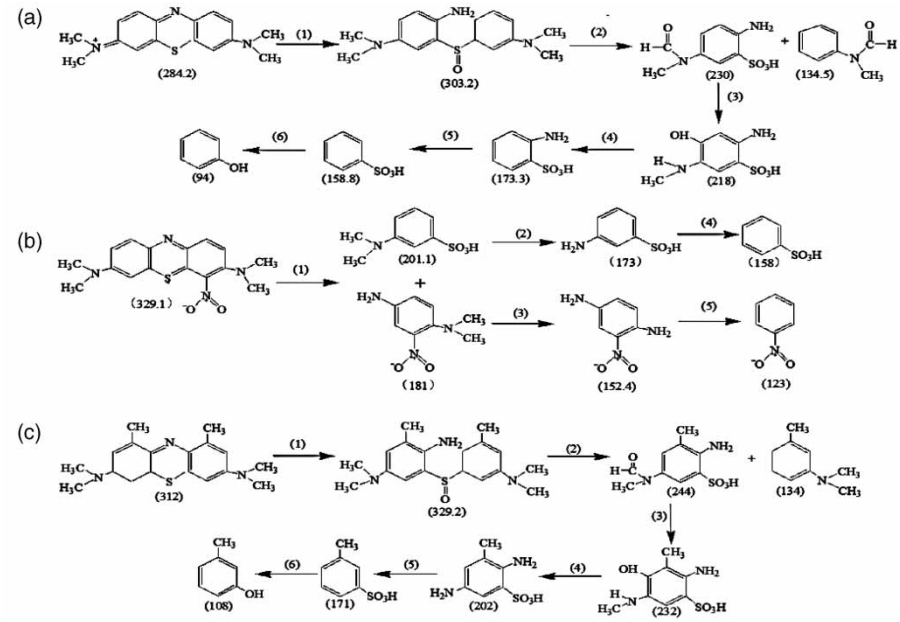

Figure 7 | Schematic diagram of photocatalytic degradation for three dye molecules: (a) methylene blue, (b) methylene green, (c) 1,9-dimethyl methylene blue.

blue. But the degradation mechanism of methylene green (Figure 7(b)) was different from that of methylene blue and 1,9-dimethyl blue. The -NH_2 group with unpaired electrons was pulled into the part containing nitro to form 2-nitro-4-amino-N,N-dimethylaniline (m/z = 181), and the main intermediate products of benzene sulfonic acid (m/z = 158) and nitrobenzene (m/z = 123) are obtained (Figure 6(b)).

CONCLUSION

We prepared graphene-doped TiO_2 microspheres by sol-gel method and used them to degrade methylene blue solution, methylene green solution and 1,9-dimethyl methylene blue solution for the first time. The corresponding photocatalysis degradation extent reached 96.4, 85.9 and 98.7% in the optimal reaction conditions, respectively. It was found that the degradation extent and photocatalytic mechanism of methylene green were different from those of methylene blue and 1,9-dimethyl methylene blue due to the withdrawing effect of the nitro functional group. The prepared composite microspheres showed great application prospects in the fields of dye wastewater treatment, environmental protection, biomedicine and so on.

NOTES

The authors declare no competing financial interests.

ACKNOWLEDGEMENT

This work was supported by the Self-financing Project of Science and Technology Research in Colleges and Universities of Hebei Province (z2018007), the Natural Science

Downloaded from http://iwaponline.com/wst/article-pdf/83/1/223/834977/wst083010223.pdf
by guest

Foundation of Hebei Province (B2019408018) and the Fundamental Research Funds for the Universities in Hebei Province (JYQ201902).

DATA AVAILABILITY STATEMENT

Data cannot be made publicly available; readers should contact the corresponding author for details.

REFERENCES

Acharya, G., Shin, C. S., Mcdermott, M., Mishra, H., Park, H., Kwon, I. C. & Park, K. 2010 The hydrogel template method for fabrication of homogeneous nano/microparticles. *Journal of Controlled Release* **141** (3), 314–319.

Anas, M., Han, D. S., Mahmoud, K., Park, H. & Abdel-Wahab, A. 2015 Photocatalytic degradation of organic dye using titanium dioxide modified with metal and non-metal deposition. *Materials Science in Semiconductor Processing* **41**, 209–218.

Bagus, P. S., Nelin, C. J., Brundle, C. R. & Chambers, S. A. 2019 A new mechanism for XPS line broadening: the 2p-XPS of Ti (IV). *Journal of Physical Chemistry C* **123** (13), 7705–7716.

Bai, W. B., Tian, X., Yao, R. J., Chen, Y. X., Lin, H. M., Zheng, J. Y., Xu, Y. L. & Lin, J. H. 2020 Preparation of nano-TiO_2@ polyfluorene composite particles for the photocatalytic degradation of organic pollutants under sunlight. *Solar Energy* **196**, 616–624.

Baschir, L., Iordache, A. M., Savastru, D., Popescu, A. A., Vasiliu, I. C., Elisa, M., Obreja, C., Filipescu, M., Trusca, R., Stchakovsky, M. & Iordache, S. 2019 Structural, morphologic and optical properties of graphene doped binary TiO_2–P_2O_5 nanocomposite. *Journal of Vacuum Science and Technology B* **37** (6), 2166–2746.

Cabir, B., Yurderi, M., Caner, N., Arta, M. S., Zahmakiran, M. & Kaya, M. 2017 Methylene blue photocatalytic degradation under visible light irradiation on copper phthalocyanine-sensitized TiO_2 nanopowders. *Materials Science and Engineering: B* **224**, 9–17.

Elma, M., Wang, D. K., Yacou, C. & Costa, J. C. D. 2015 Interlayer-free P123 carbonised template silica membranes for desalination with reduced salt concentration polarisation. *Journal of Membrane Science* **475** (1), 376–383.

Ette, P. M., Selvakumar, K., Senthil, K. S. M. & Ramesha, K. 2018 Silica template assisted synthesis of ordered mesoporous β–MnO_2 nanostructures and their performance evaluation as negative electrode in Li-ion batteries. *Electrochimica Acta* **292** (1), 532–539.

He, P. J., Huang, L. H., Wu, X. Y., Xu, Z., Zhu, M. Y., Wang, X. G. & Dai, B. 2018 A novel high-activity Zn-Co catalyst for acetylene acetoxylation. *Catalysts* **8**, 239.

Juma, A., Acik, I. O., Oluwabi, A. T., Mere, A., Mikli, V., Danilson, M. & Krunk, M. 2016 Zirconium doped TiO_2 thin films deposited by chemical spray pyrolysis. *Applied Surface Science* **387** (30), 539–545.

Kim, S. R., Ali1, I. & Kim, J. O. 2017 Phenol degradation using an anodized graphene-doped TiO_2 nanotube composite under visible light. *Applied Surface Science* **37984**, 1–8.

Kim, S. J., Chang, H., Choi, J. Y., Song, Y. J. & Heller, M. J. 2019 Ultrathin sub-3 nm nitrogen-doped graphene quantum dot layers coated TiO_2 nanocomposites as high-performance photocatalysts. *Chemical Physics Letters* **714**, 1–5.

Li, S. S., Qian, K. K., Wang, S., Liang, K. Q. & Yan, W. 2017 Polypyrrole-grafted coconut shell biological carbon as a potential adsorbent for methyl tert-butyl ether removal: characterization and adsorption capability. *International Journal of Environmental Research and Public Health* **14**, 113.

Liu, S. W., Yu, J. G. & Jaroniec, M. 2010 Tunable photocatalytic selectivity of hollow TiO_2 microspheres composed of anatase polyhedra with exposed {001} facets. *Journal of the American Chemical Society* **132** (34), 11914–11916.

Liu, Y. W., Teitelboim, A., Bravo, A. F., Yao, K. Y., Virginia, M., Altoe, P., Aloni, S., yuan, A., Zhang, C. H., Cohen, B. E., Schuck, P. J. & Chan, E. M. 2020 Controlled assembly of upconverting nanoparticles for low-threshold microlasers and their imaging in scattering media. *ACS Nano* **14** (2), 1508–1519.

Michael, I., Hapeshi, E., Michael, C. & Fatta-Kassinos, D. 2013 Superiority of solar Fenton oxidation over TiO_2 photocatalysis for the degradation of trimethoprim in secondary treated effluents. *Water Science & Technology* **67** (6), 1260–1271.

Nador, F., Guisasola, E., Baeza, A., Moreno- Villaecija, M. A., Vallet-Regí, M. & Ruiz-Molina, D. 2017 Synthesis of polydopamine-like nanocapsules via removal of a sacrificial mesoporous silica template with water. *Chemistry – A European Journal* **23** (12), 2733–2733.

Nappini, S., Matruglio, A., Naumenko, D., Zilio, S. D., Bondino, F., Lazzarino, M. & Magnano, E. 2017 Graphene nanobubbles on TiO_2 for *in-operando* electron spectroscopy of liquid-phase chemistry. *Nanoscale* **9** (13), 4456–4466.

Nguyen, L. T., Lee, K. H. & Lee, B. T. 2011 A novel photoactive nano-filtration module composed of a TiO_2 loaded PVA nano-fibrous membrane on sponge Al_2O_3 scaffolds and Al_2O_3-(m-ZrO_2)/t-ZrO_2 composites. *Materials Transactions* **52** (7), 1452–1456.

Pal, N., Cho, E. B., Kim, D. & Jaroniec, M. 2014a Mn-doped ordered mesoporous ceria-silica composites and their catalytic properties toward biofuel production. *The Journal of Physical Chemistry C* **118** (29), 15892–15901.

Pal, S., Patra, A. S., Ghorai, S., Sarkar, A. K. & Sarkar, S. 2014b Modified guar gum/TiO_2: development and application of a novel hybrid nanocomposite as a flocculant for the treatment of wastewater. *Environmental Science Water Research & Technology* **1** (1), 84–95.

Pant, B., Park, M. & Park, S. J. 2020 Hydrothermal synthesis of Ag_2CO_3-TiO_2 loaded reduced graphene oxide nanocomposites with highly efficient photocatalytic activity. *Chemical Engineering Communications* **207** (5), 688–695.

Pare, B., Solanki, V. S., Gupta, P. & Jonnalgadda, S. B. 2016 Visible-light induced photocatalytic mineralization of

Downloaded from http://iwaponline.com/wst/article-pdf/83/1/223/834977/wst083010223.pdf
by guest

methylene green dye using $BaCrO_4$ photocatalyst. *Indian Journal of Chemical Technology* **23** (6), 513–519.

Pham, T. N., Shi, D. & Resasco, D. E. 2014 Reaction kinetics and mechanism of ketonization of aliphatic carboxylic acids with different carbon chain lengths over Ru/TiO_2 catalyst. *Journal of Catalysis* **314**, 149–158.

Shakeel, M., Jabeen, F., Shabbir, S., Asghar, M. S., Khan, M. S. & Chaudhry, A. S. 2016 Toxicity of nano-titanium dioxide (TiO_2-NP) through various routes of exposure: a review. *Biological Trace Element Research* **172** (1), 1–36.

Shinde, Y., Wadhai, S., Ponkshe, A., Kapoor, S. & Thakur, P. 2018 Decoration of Pt on the metal free RGO-TiO_2 composite photocatalyst for the enhanced photocatalytic hydrogen evolution and photocatalytic degradation of pharmaceutical pollutant β blocker. *International Journal of Hydrogen Energy* **43** (8), 4015–4027.

Tang, H., Zhang, D., Tang, G. G., Ji, X. R., Li, W. J., Li, C. S. & Yang, X. F. 2013 Hydrothermal synthesis and visible-light photocatalytic activity of α-Fe_2O_3/ composite hollow microspheres. *Ceramics International* **39** (8), 8633–8640.

Wang, P. Q., Bai, Y. & Liu, J. Y. 2013 Photocatalytic degradation of phenol using Au/Bi_2WO_6 composite microspheres under visible-light irradiation. *Micro & Nano Letters* **8** (2), 90–93.

Wei, D. C., Liu, Y. Q., Zhang, H. L., Huang, L. P., Wu, B., Chen, J. Y. & Yu, G. 2009 Scalable synthesis of few-layer graphene ribbons with controlled morphologies by a template method and their applications in nanoelectromechanical switches. *Journal of the American Chemical Society* **131** (31), 11147–11154.

Xiao, F. Y., Ren, H., Zhou, H. S., Wang, H. Z., Wang, N. & Pan, D. W. 2019 Porous montmorillonite@graphene oxide@Au nanoparticle composite microspheres for organic dye degradation. *ACS Applied Nano Materials* **2** (9), 5420–5429.

Yang, C. C., Doong, R. A., Chen, K. F., Chen, G. S. & Tsai, Y. P. 2018 The photocatalytic degradation of methylene blue by green semiconductor films that is induced by irradiation by a light-emitting diode and visible light. *Journal of the Air & Waste Management Association* **68** (1), 29–38.

Yu, M. P., Ma, J. S., Song, H. Q., Wang, A. J., Tian, F. Y., Wang, Y. S., Qiu, H. & Wang, R. M. 2016 Atomic layer deposited TiO_2 on a nitrogen-doped graphene/sulfur electrode for high performance lithium-sulfur batteries. *Energy & Environmental Science* **9** (4), 1495–1503.

Zhang, Q. S. & Zhang, Z. K. 2009 Preparation and characterization of nanocrystalline Fe-doped TiO_2 film on different substrates and its application in degrading dyeing water. *Journal of Dispersion Science and Technology* **30** (1), 110–114.

Zhang, J., Wang, W. Z., Zhang, X. R., Zheng, X. & Wu, Z. C. 2015 Enhanced antifouling behaviours of polyvinylidene fluoride membrane modified through blending with nano-TiO_2/ polyethylene glycol mixture. *Applied Surface Science* **345** (1), 418–427.

Zhi, L. J., Gorelik, T., Wu, J. S., Kolb, U. & Muellen, K. 2005 Nanotubes fabricated from Ni naphthalocyanine by a template method. *Journal of the American Chemical Society* **127** (37), 12792–12793.

First received 31 July 2020; accepted in revised form 27 October 2020. Available online 12 November 2020

Downloaded from http://iwaponline.com/wst/article-pdf/83/1/223/834977/wst083010223.pdf
by guest